

# **VT/NASA BeVERLI Hill Smooth Wall Separation Over Bumps**

Version 1: 27 October 2020

## **Test Case Coordinators**

Todd Lowe, William Devenport, Chris Roy, and Aurelien Borgoltz

Virginia Tech, US

E-mail : [kelowe@vt.edu](mailto:kelowe@vt.edu); [devenport@vt.edu](mailto:devenport@vt.edu); [cjroy@vt.edu](mailto:cjroy@vt.edu); [aborgolt@vt.edu](mailto:aborgolt@vt.edu)

Phone: (540) 231-7650

Student Contacts: Julie Duetsch-Patel and Aldo Gargiulo

Virginia Tech, US

E-mail: [juliedp@vt.edu](mailto:juliedp@vt.edu); [galdo@vt.edu](mailto:galdo@vt.edu)

## **I. Introduction**

The objectives of this experiment are to measure the smooth wall, high Reynolds number, boundary layer flow over a bump model (the BeVERLI Hill) to generate a database of experimental results for CFD validation studies. This experiment is conducted in the closed-circuit, subsonic Virginia Tech Stability Wind Tunnel. The experimental setup involves a fifth-degree polynomial bump model that can be positioned at various orientations to generate different flows over the body. Schematics of the bump and of the tunnel setup are shown in Figures 1 and 2 and are accompanied by an explanation of the coordinate system in Section IV below. The following sections are intended to communicate the available data content and their file formats.

## **II. BeVERLI Hill As-Designed Geometry**

The description of the bump geometry is adapted from Lowe et al. [1]. Additional details are available in Gargiulo et al.

A novel and fully analytic bump geometry has been developed for this study (see Figure 1). It is generated by requiring continuous curvature in all three dimensions, while allowing for flat sections on the four sloping sides and a flat top, ideal for optical diagnostics access. A fifth-order polynomial provides enough parameters to meet these conditions for generating the curved sections fairing to the floor and to the flat top. The four sloping sides yield continuous curvature by creating corners described by a superellipse with exponent equal to 4. Note, the initial design of the bump geometry was performed utilizing Imperial units and is now reported in these units

throughout this description of the bump geometry to avoid the introduction of round-off inaccuracies from converting bump geometry parameters to SI units. Reporting these parameters exactly as designed, using Imperial units, will assure a higher accuracy when attempting to recreate this geometry from the test case description.

The bump scaling is based on the tunnel geometry and tunnel boundary layer scales. Specifically, the boundary layer thickness  $\delta = 63$  mm at the center of the test section and the flow conditions are set by Reynolds number, where the maximum height-based Reynolds number,  $Re_h = 650K$ , corresponding to a nominal free-stream velocity of  $U_\infty = 55$  m/s and Mach number of  $M_\infty = 0.16$ . Furthermore, a bump width-to-boundary layer thickness ratio  $w/\delta = 14$  and a bump height to boundary layer thickness ratio  $h/\delta = 3$  are selected as desired values for the bump geometry design. The choice of the latter features was informed by already existing studies of bump flow conducted by other research groups and were thought to place the study in the proper parameter space for achieving three separation regimes (attached flow, incipient separation, and massive smooth-body turbulent separation) on varying parts of the bump or at varying orientations. Given all the above and taking into account limitations imposed by the manufacturing of the physical bump model, a bump width of  $w = 36.8$  in  $= 0.93472$  m and a bump height of  $h = 7.36$  in  $= 0.186944$  m are selected.

The 2D centerline cross-section of the full 3D bump geometry is represented by the connection of two mirrored 5th degree polynomial profiles  $P_5(x)$  with a flat top. Considering the coordinate system in Figure 2, the polynomial is first fitted on the positive x-axis imposing the 6 polynomial constraints depicted in Table 1. Note, these constraints impose a zero-slope and zero-curvature condition at the boundaries of the polynomial. The generated polynomial profile face is mirrored about the  $x = 0$  axis to form the opposite face of the bump on the negative x-axis. A flat top of length  $s = 3.68$  in  $= 0.093472$  m connects the two polynomial faces to form the complete 2D bump profile shown in Figure 1, where the polynomial faces are depicted by a blue curve and the flat top by a red curve.

To generate the complete 3D bump geometry, the 2D profile is first extruded spanwise a length of  $s/2$  both along the positive and the negative y-axis. This creates a straight cylindrical body of thickness  $s$ , which is represented in Figure 1 by red and blue shaded surfaces. The colored dashed line at the center of the shaded surfaces, hereby, symbolizes the 2D bump profile through the centerline of the 3D geometry. The cylindrical section is rotated by 90 degrees in the

mathematical positive sense about the z-axis to generate the aforementioned 90 degrees rotational symmetry. This rotation also generates a squared flat top, which is highlighted by a red solid line in Figure 1. This flat top further facilitates optical flow measurements on the surface of the bump such as PIV and LDV. The corners of the bump are completed by rotating the  $P_5(x)$  polynomial face about each corner of the flat top, constraining the rotation by a superelliptic curve at the bump base. In Figure 1, the corners are labeled as  $C_i$  for  $i = 1, 2, 3, 4$ . The superelliptic curve is parametrized using an angle parameter  $t$ . The respective parametrization is

$$x_i = \frac{b_i}{2} + |\cos(t)|^{\frac{1}{2}} \cdot \frac{w-s}{2} \cdot \text{sgn}(\cos(t)) \quad (1)$$

$$y_i = \frac{c_i}{2} + |\sin(t)|^{\frac{1}{2}} \cdot \frac{w-s}{2} \cdot \text{sgn}(\sin(t)) \quad (2)$$

where the parameters in these equations are provided in Table 3.

The attributes of the bump geometry mentioned above have been specified deliberately and with special attention to the unique demands of validation and turbulence model development experiments. First, the bump configuration lends itself to simple parametric variations important to this program. By scaling the bump width and the size of the oncoming boundary layer, the size of the separation region can be increased or reduced. Specifically it can be reduced to the point of achieving a flow characterized only by incipient separation and attached flow. Importantly, the dashed lines in fig. 6 depict the boundaries of cylindrical sections of the geometry. These features are critical for enabling a practical means for manufacturing and installing optical windows and instrumentation inserts into the bump. Importantly, the cylindrical windows will allow for the documentation of boundary layer details not just in the separated flow region, but also in the critical regions of the attached nonequilibrium turbulent boundary layer leading up to separation. These data will be immediately useful for diagnosing modeling shortcomings that lead to discrepancies in the separated flow region. Lastly, unlike most other bump configurations, the analytic geometry is exactly flat at the edges of the geometry, while curvature varies smoothly from zero up the sides. This feature will reduce or eliminate physical complexities associated with propagating boundary layer characteristics arising from edge curvature discontinuities.

The as-tested geometry of the bump model will be available in the form of point clouds extracted from laser scans made with a resolution of  $1.2 \text{ mm}$  and accuracy of  $\pm 2 \text{ mm}$  at  $10 \text{ m}$  measuring distance.

### III. Nominal Test Conditions

While more detailed test conditions will be provided in the near-term, these nominal test conditions are provided to facilitate simulation setup in the interim. The ideal gas law can be used to compute the density and Sutherland's relation can be used to compute the viscosity.

| <b>Re<sub>H</sub></b> | <b>Inlet Total Pressure</b> | <b>Total Temperature</b> | <b>Outlet Static Pressure</b> |
|-----------------------|-----------------------------|--------------------------|-------------------------------|
| <b>325,000</b>        | 94,300 Pa                   | 287 K                    | 93,869 Pa                     |
| <b>487,500</b>        | 94,300 Pa                   | 287 K                    | 93,257 Pa                     |
| <b>650,000</b>        | 94,300 Pa                   | 287 K                    | 92,616 Pa                     |

### IV. Coordinate System and Nominal Geometry

This section explains the coordinate system implemented in the smooth wall experiments. Provided below are nominal (as-designed) geometric conditions of the VT SWT setup. The as-tested geometry of the test section and contraction will be available in the form of point clouds extracted from laser scans made with a resolution of 1.2 mm and accuracy of  $\pm 2$  mm at 10 m measuring distance.

| <b>File Name</b>              | <b>Description and Content</b>  |
|-------------------------------|---|
| <i>VT_EmptyTestSection_v3</i> | ○ As designed CAD of the empty test section.  |
| <i>Contraction_NATO_v2</i>    | ○ As designed CAD of the contraction liner. Note that the “transition panel” geometry between the test section cross section and contraction exit is not included at this time. |
| <i>BeVERLI_Hill</i>           | ○ As designed CAD of the BeVERLI Hill model.  |

#### General Notes:

- The test section cross section is 1.848 m x 1.848 m and is 7.315 m in length.

#### Coordinate System:

- Right-hand coordinate system (see Figures 3 and 4)
- The port side wall is treated as the “ground,” and is used to grow the boundary layer that is the focus of this study.

- The origin of the  $x, y, z$  coordinate system is the point on the port side wall, at its mid height, at the seam denoting the downstream end of the transition from the contraction, as illustrated in Figure 2. This point is nominally  $3.584m$  downstream of the trip location and  $3.54m$  upstream of the airfoil quarter chord location, measured along the tunnel axis.
- The  $x$  coordinate is measured downstream along the test section axis from the origin (see Figure 2). In the attached *VT\_EmptyTestSection\_v3*, showing the nominal test geometry, the  $x = 0$  plane is labeled as “ $x=0$ ”, at a position  $0.110m$  downstream of the leading edge of the rectangular cuboid shown in the CAD. This coordinate represents the streamwise direction of flow.
- The coordinate  $y$  is measured perpendicular from the port-side test section wall into the flow. In experimental data,  $y = 0$  represents the wall position and thus implicitly assumes that the wall is planar and passes through the coordinate system origin. Departures from this assumption will be detailed in later data releases to include as-measured geometry scans of the tunnel wall.
- The coordinate  $z$  is measured parallel to the port-side test section wall, in the spanwise direction so as to complete a right handed system. In the attached nominal geometry file *VT\_EmptyTestSection\_v3*, this is represented by the plane labeled as “ $z=0$ ”, which is equidistant by  $0.924 m$  from the floor and ceiling.
- Inflow measurements are made in the plane at  $x = 1.16 m$ .

#### BeVERLI Hill

- The center of the BeVERLI model is nominally  $3.30 m$  from the  $x = 0$  point of reference (streamwise distance).

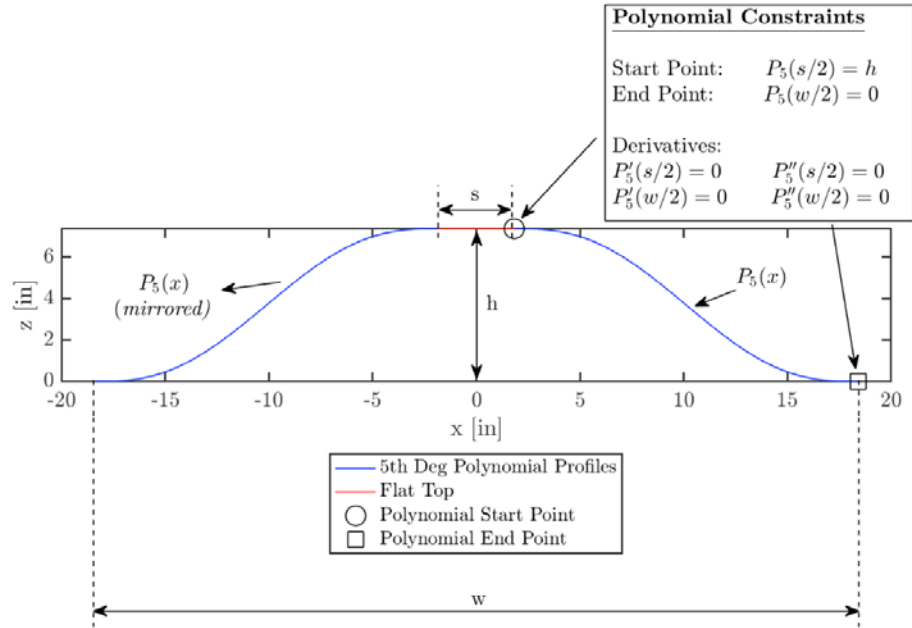
#### Contraction Liner (see Figure 4)

- Flow exits the settling chamber and is accelerated by a 9:1 ratio contraction section.
- The *Contraction\_NATO\_v2* represents only  $4.032m$  of the entire contraction. This distance is only the contraction liner profile that was installed in the VT SWT [2].
- The transition panel between the contraction exit and test section entrance extends approximately  $0.5m$  in the streamwise direction, on the port wall. Exact curvature and dimensions of the contraction/test section interface will be made available with the tunnel scan data (estimated availability – August 2020).

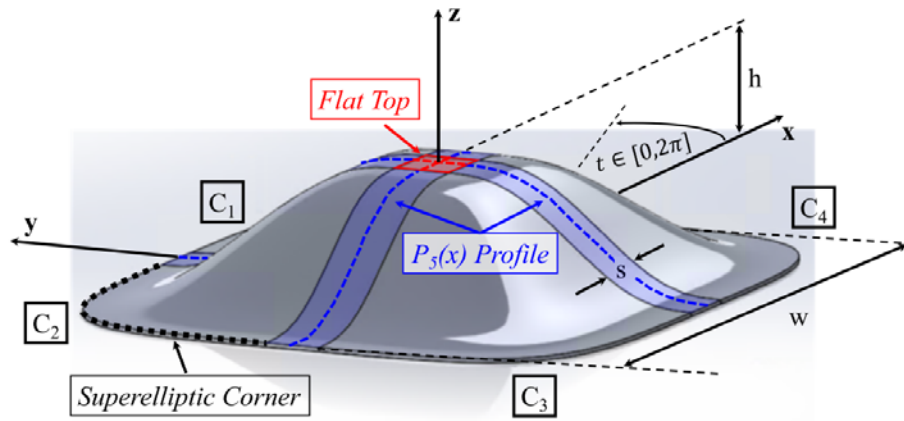
- The boundary layer is tripped in the wind tunnel contraction, upstream of the test section entrance at  $x = -3.58m$ . The trip has a 27.6-degree zig-zag planform pattern periodic on 10 mm with a total height of 3.18 mm and a total streamwise width of 20.39 mm.

#### IV. References

- [1] Lowe, T., Beardsley, C., Borgoltz, A., Devenport, W. J., Duetsch-Patel, J. E., Fritsch, D. J., Gargiulo, A., Roy, C. J., Szoke, M., and Vishwanathan, V. "Status of the NASA/Virginia Tech Benchmark Experiments for CFD Validation." *AIAA SciTech 2020 Forum*, Orlando, FL, Jan 6, 2020., AIAA 2020-1584.
- [2] Vishwanathan, V., Szoke, M., Duetsch-Patel, J. E., Totten, E. D., Gargiulo, A., Fritsch, D. J., Borgoltz, A., Roy, C. J., Lowe, K. T., and Devenport, W. J. "Aerodynamic Design and Validation of a Contraction Profile for Flow Field Improvement and Uncertainty Quantification in a Subsonic Wind Tunnel." *AIAA SciTech 2020 Forum*, Orlando, FL, Jan 6, 2020., AIAA 2020-2211.



(a) 2D Bump Design - 5th Degree Polynomial Bump Faces Profile



(b) 3D Bump Design

Figure 1. BeVERLI Hill designed geometry.

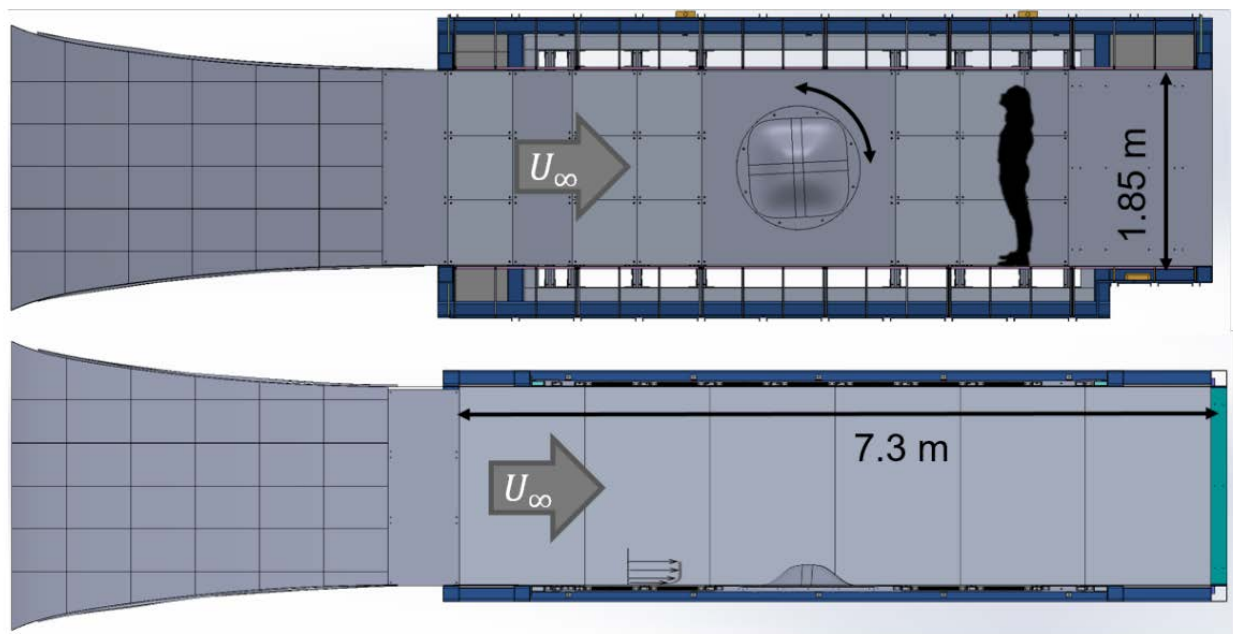


Figure 2. Schematic of test section and contraction liner as-designed configuration with BeVERLI Hill installed on the port wall (mirrored to show flow from L->R).

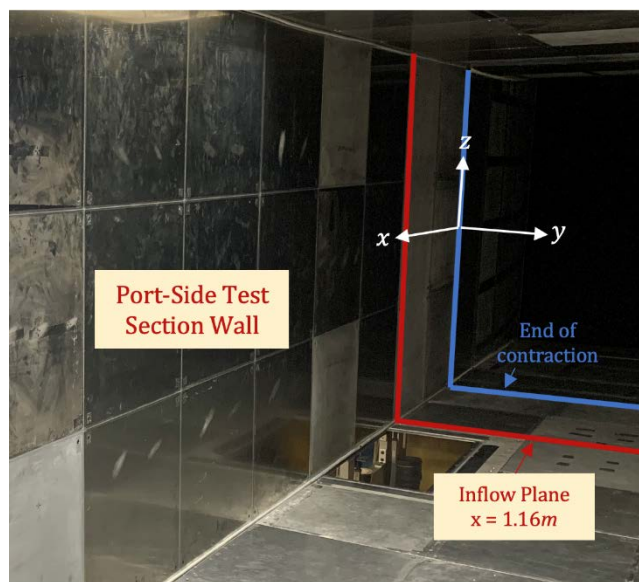


Figure 3. Downstream view of partial port wall without bump installed. This figure is intended to show to the coordinate system and inflow plane references.



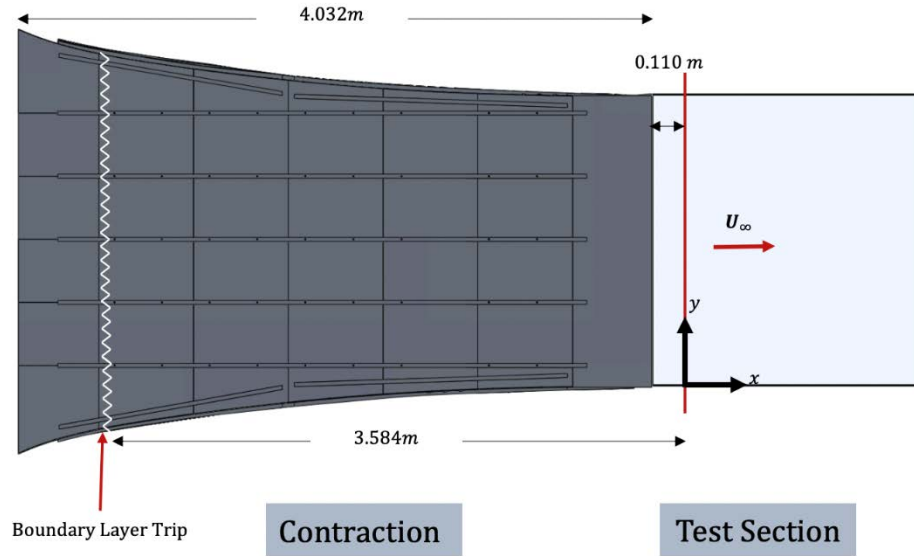


Figure 4. Top-down schematic of the contraction liner interface with the entrance of the test section. Outer view of contraction is shown with ribs and modular panels. Note that the boundary layer trip is visually represented and is not to scale.

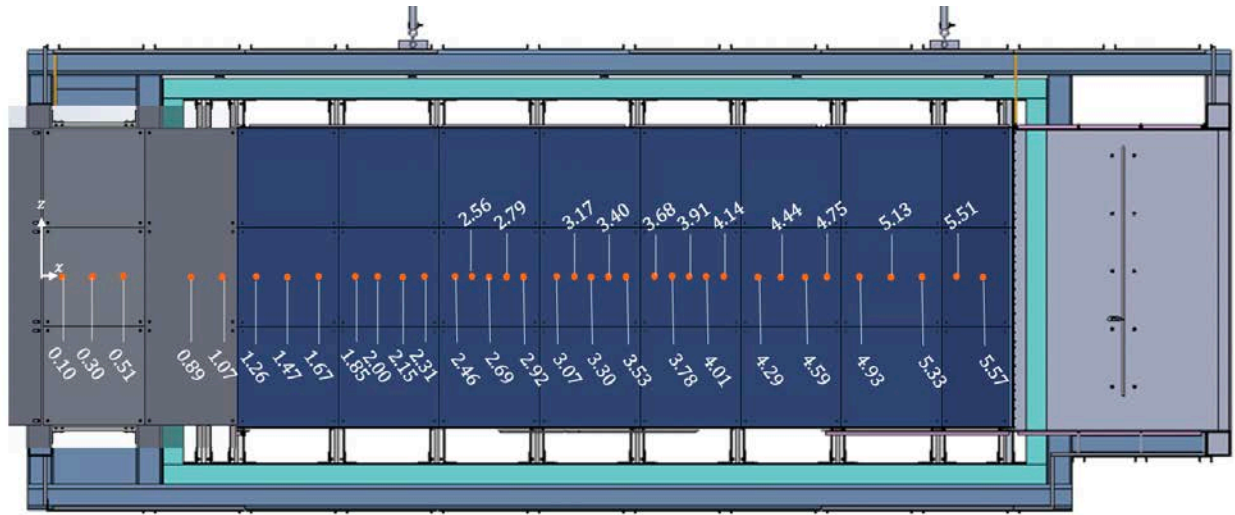


Figure 5. STARBOARD test section wall pressure tap distribution (in meters) is shown;  $(y, z) = (0 \text{ m}, 0 \text{ m})$ . Port wall tap distribution is nominally identical in the streamwise ( $x$ ) direction;  $(y, z) = (0 \text{ m}, 1.848 \text{ m})$ . Flow is left to right.

Table 1. 5<sup>th</sup> degree polynomial constants.

|                 |                  |                  |
|-----------------|------------------|------------------|
| Function:       | $P_5(s/2) = h$   | $P_5(w/2) = 0$   |
| 1st Derivative: | $P'_5(s/2) = 0$  | $P'_5(w/2) = 0$  |
| 2nd Derivative: | $P''_5(s/2) = 0$ | $P''_5(w/2) = 0$ |

Table 2.  $P_5(x)$  coefficients in Imperial units (inches<sup>1-m</sup>, where  $m$  is the polynomial coefficient subscript).

| $z(x) = P_5(x) = a_5x^5 + a_4x^4 + a_3x^3 + a_2x^2 + a_1x + a_0$ $x \in \left[\frac{s}{2}, \frac{w}{2}\right]$ |  |
|--|--|
| $a_5$  | $-35.459\,075\,020\,286\,8 \times 10^{-6}$ |
| $a_4$  | $1.794\,229\,196\,026\,51 \times 10^{-3}$  |
| $a_3$  | $-28.211\,807\,431\,340\,5 \times 10^{-3}$ |
| $a_2$  | $121.490\,847\,321\,347 \times 10^{-3}$    |
| $a_1$  | $-203.221\,053\,701\,163 \times 10^{-3}$   |
| $a_0$  | $7.478\,534\,776\,202\,81$                 |

Table 3. Parameterization coefficients.

|         | Corner $C_1$         | Corner $C_2$           | Corner $C_3$            | Corner $C_4$             |
|---------|----------------------|------------------------|-------------------------|--------------------------|
| $i =$   | 1                    | 2                      | 3                       | 4                        |
| $b_i =$ | s                    | -s                     | -s                      | s                        |
| $c_i =$ | s                    | s                      | -s                      | -s                       |
| $t \in$ | $[0, \frac{\pi}{2}]$ | $[\frac{\pi}{2}, \pi]$ | $[\pi, \frac{3\pi}{2}]$ | $[\frac{3\pi}{2}, 2\pi]$ |